Damage spreading in a two-dimensional Potts ferromagnet in an external field

1997 J. Phys. A: Math. Gen. 30 2329

(http://iopscience.iop.org/0305-4470/30/7/014)

J. Phys. A: Math. Gen. **30** (1997) 2329–2344. Printed in the UK PII: S0305-4470(97)77990-3

Damage spreading in a two-dimensional Potts ferromagnet in an external field

L da Silva†§, F A Tamarit‡‖ and A C N Magalhães†¶

† Centro Brasileiro de Pesquisas Físicas - CBPF, Rua Dr Xavier Sigaud, 150 22290-180 Rio de Janeiro, RJ, Brazil

‡ FaMAF, Universidad Nacional de Córdoba, Ciudad Universitaria, 5000 Córdoba, Argentina

Received 19 September 1996, in final form 31 December 1996

Abstract. We study, using the damage spreading method and within the heat bath dynamics, the dynamical behaviour of the square lattice three-state Potts ferromagnet subjected to an external field. In the zero field case, we verify that this very simple model presents, besides the transition consistent with the equilibrium one, a new dynamical chaotic phase with unusual features. Although the unexpected transition occurs, within the error bars, at the static Ising critical temperature, it is in the directed percolation universality class. We observe that the application of a uniform magnetic field does not destroy any of the two transitions, while the unexpected one is annihilated by a new kind of field which plays the role of a conjugate field to the Hamming distance.

1. Introduction

The damage spreading technique [1–22] has been greatly employed in the study of time-dependent critical phenomena in spin systems. In this method one essentially monitors the time evolution of two or more copies of the same system with different initial configurations subjected to a specific dynamics and to the *same* thermal noise. The usual monitored quantity is the Hamming distance or *damage*, $D(t)$, defined as the fraction of elements which differ between the two configurations. The variation of the damage and related quantities with time, temperature, initial conditions and any other relevant parameter leads to information about the criticality of the system.

The results from the damage spreading process can be quite different for distinct dynamics (see, for example [21]). For instance, in the Ising ferromagnet the spreading transition seems to coincide with the static critical temperature [2–4, 17] if one uses the heat-bath dynamics, while the opposite happens within the Glauber stochastic process [7, 18].

In more complex systems, such as the two-dimensional (2D) anisotropic next-nearest neighbour Ising (ANNNI) model [3], the three-dimensional (3D) and mean-field spin glasses [2, 10, 16], the 2D XY ferromagnet [5], the 3D Heisenberg model [13], the p-state ($5 \leqslant p \leqslant 10$) clock model [12] and a soluble dilute ferromagnetic model [11], it has found more than two dynamical phases where a few of them have no clearly known static equivalent. In the 3D spin glasses within the heat-bath dynamics [2, 10] and the 2D XY

§ E-mail address: ladario@cat.cbpf.br
‖ E-mail address: tamarit@fis.uncor.edu
¶ E-mail address: aglae@cat.cbpf.br

0305-4470/97/072329+16$19.50

ferromagnet within the Metropolis dynamics [5], three different regimes were obtained where the lower transition temperature seems to agree with the equilibrium one, and it corresponds to the temperature above which the damage looses its dependence on the initial damage. The upper transition temperature (above which the damage vanishes) is consistent, in the case of spin glasses, with the temperature below which stretched exponential relaxations start to appear [23, 24].

All systems with three or more dynamical phases that have been studied so far have some complex features, such as competing interactions, dilution, continuous symmetry, non-trivial discrete symmetry (Z_q for $q \geqslant 5$), etc. One, then, may pose the question whether this would be possible in a system without such degree of complexity. We verify herein, through the damage spreading technique, that *a very simple model*, namely the square lattice three-state Potts ferromagnet subjected to the usual heat-bath dynamics, has a *three-phase structure*. Its corresponding static model has been extensively studied (for a review on the q-state Potts model see [25]) and, in particular, it has a continuous para-ferromagnetic phase transition at the exact critical temperature $k_B T_c(q = 3)/J = [\ln(1 + \sqrt{3})]^{-1}$ with precisely determined critical exponents. Much less is known about its dynamics. In particular, a lot of emphasis has been given to the determination of the dynamic critical exponent, z, calculated at the dynamical transition which occurs at the mentioned equilibrium T_c. The region above T_c has not, to our knowledge, been explored such that one could guarantee that there is no change of regime in this region. Notice also that the investigation of the dynamical behaviour of the Potts model through the damage spreading technique has not been published†.

Another interesting point which has hardly been investigated is the identification of the conjugate field associated with continuous dynamical transitions. It has been found [7, 18] in the 2D and 3D Ising ferromagnet subjected to the Glauber dynamics, that an external uniform magnetic field, B, does not destroy the damage transition. Recently, two of us [15] have verified that a new kind of external field, h, introduced in literature [28] in the context of cellular automata (see also [29] for a mean-field version of it), plays the role of a conjugate field to the Hamming distance in the case of the Ising ferromagnet subjected to the heat-bath stochastic process. This field is defined as the frequency at which different random numbers are used for updating the two replicas. We also study, in this paper, the influences of both external fields, B and h, on the dynamical transitions of the 2D three-state Potts ferromagnet.

The outline of this paper is as follows. In section 2 we describe the above model and the spreading of damage method which we use. In section 3 we present our results in a zero field, while in section 4 we study the influence of external fields on the dynamical phase diagram. Finally, the conclusions are given in section 5. Notice that a short account of part of the zero field results has already been reported [30].

2. Model and method

Let us associate with each site, i, of the square lattice a Potts variable, σ_i, which can assume $q = 3$ integer values ($\sigma_i = 0, 1$and 2) and consider the Potts ferromagnet model described by the following Hamiltonian:

$$H = -J \sum_{\langle ij \rangle} \delta(\sigma_i, \sigma_j) - B \sum_i \delta(\sigma_i, 0) \qquad (\sigma_i = 0, 1, 2, \ldots, q-1) \qquad (1)$$

† We have learnt of two related works in progress [26, 27], one of them [26] studying the appearance of first-order dynamical transitions for higher values of the number of q-states.

where $J > 0$ is the ferromagnetic coupling constant between nearest-neighbour spins, B is an external homogeneous magnetic field applied to the state $\sigma_i = 0$, and $\delta(\sigma_i, \sigma_j)$ is the Kronecker delta function. The first sum is over all the nearest-neighbour spins $\langle ij \rangle$, while the second one is over all sites, i, of the square lattice.

Later on, instead of a magnetic field, we shall apply the above mentioned external field, h, in order to check whether it destroys any of the transitions at $h = 0$ and whether it leads to the divergence of its associated susceptibility at its transition temperature.

Our numerical simulations are implemented on squares with N spins and linear size $L(N = L^2 \text{sites})$ submitted to periodic boundary conditions. To update the spin variables we use a sequential Monte Carlo heat-bath process (in a fully vectorized code). At each Monte Carlo step (MCS) t and for a given spin $\sigma_i(t)$ at site i, we first compute the energy differences $\Delta E_i^{\alpha\beta}(t) = E_i^{\beta} - E_i^{\alpha}$ for changing the spin $\sigma_i(t)$ at the state α into the state $\beta(\alpha, \beta = 0, 1, 2)$, and afterwards calculate the probabilities $p_i^{(\alpha)}(\alpha = 0, 1, 2)$ for $\sigma_i(t+1)$ to be in the state α, namely:

$$p_i^{(0)} = [1 + \exp(-\beta \Delta E_i^{(01)}) + \exp(-\beta \Delta E_i^{(02)})]^{-1} \tag{2}$$

$$p_i^{(1)} = [1 + \exp(\beta \Delta E_i^{(01)}) + \exp(-\beta \Delta E_i^{(12)})]^{-1} \tag{3}$$

$$p_i^{(2)} = [1 + \exp(\beta \Delta E_i^{(02)}) + \exp(\beta \Delta E_i^{(12)})]^{-1} = 1 - p_i^{(0)} - p_i^{(1)} \tag{4}$$

where $\beta = 1/k_B T$ and T is the temperature of the system. The new state $\sigma_i(t+1)$ of the spin, σ_i, is then determined by comparing a chosen pseudo-random number $r_i(t) \in [0, 1]$ with the above probabilities according to the following rule:

$$\sigma_i(t+1) = \begin{cases} 0 & \text{if } r_i(t) \leqslant p_i^{(0)} \\ 1 & \text{if } p_i^{(0)} < r_i(t) \leqslant p_i^{(0)} + p_i^{(1)} \\ 2 & \text{if } p_i^{(0)} + p_i^{(1)} < r_i(t) \leqslant 1. \end{cases} \tag{5}$$

Let us consider two different initial configurations, $\{\sigma_i^{(A)}(0)\}$ and $\{\sigma_i^{B}(0)\}$, at time $t = 0$ and let them evolve according to the above dynamics submitted to the *same* thermal noise, i.e. using the same sequence of random numbers for updating the spins. We shall compare the two configurations, $\{\sigma_i^{A}(t)\}$ and $\{\sigma_i^{B}(t)\}$, through the following distance $D(t)$ between them:

$$D(t) = \frac{1}{N} \sum_{i=1}^{N} [1 - \delta(\sigma_i^{A}(t), \sigma_i^{B}(t))] \tag{6}$$

where the sum is over all the N sites. Defined in this way, $D(t)$ is the fraction of spins which differs in the two replicas at time t.

In order to average $D(t)$ over thermal fluctuations we repeat the simulations for M samples, which leads to the average damage $\langle D(t) \rangle$:

$$\langle D(t) \rangle = \lim_{M \to \infty} \frac{\sum_{s=1}^{M} D_s(t)}{M} \tag{7}$$

where $D_s(t)$ is the distance measured at time, t, for the sth sample.

If two configurations become identical at time, t, they will remain identical for all later times since they are updated with the same sequence of random numbers. Consequently we can introduce the *survival probability*, $P(t)$, of two configurations remaining different at time, t, given by

$$P(t) = \lim_{M \to \infty} \frac{M_1(t)}{M} \tag{8}$$

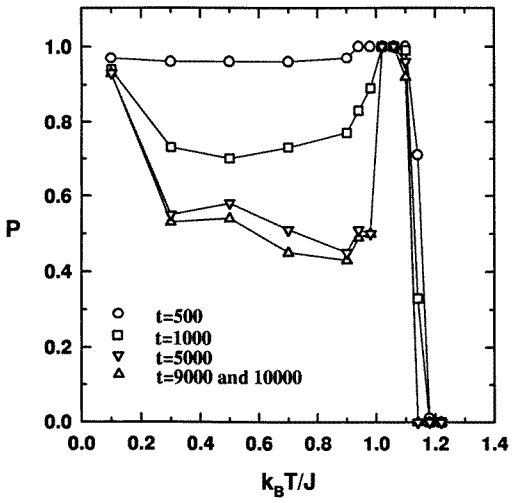

Figure 1. The survival probability, $P(t)$, versus temperature for different values of time. The data for $t = 9000$ and 10 000 coincide within the scale used. $M = 100$ samples of linear size $L = 64$ with set (c) of the initial configurations (where $D(0) = 0.05$) were examined.

where $M_1(t)$ is the number of samples such that $\{\sigma_i^A(t)\}$ and $\{\sigma_i^B(t)\}$ are still different at time t. Therefore, we can rewrite (7) as

$$\langle D(t)\rangle = \langle d(t)\rangle P(t) \tag{9}$$

where $\langle d\rangle$ is measured over only those $M_1(t)$ samples which have survived.

Throughout this paper we consider principally three different sets of initial configurations for the two replicas, namely

(a) ordered along distinct states: $\{\sigma_i^A(0) = 0, \forall_i\}$ and $\{\sigma_i^B(0) = 1, \forall_i\}(D(0) = 1)$;

(b) configuration $\{\sigma_i^A(0)\}$ is random and configuration $\{\sigma_i^B(0)\} = \{\sigma_i^A(0)\}$ except for 50% of the spins which are randomly chosen and given any of the two other possible states with equiprobability $(D(0) = \frac{1}{2})$;

(c) same as in (b) except for 5% of the chosen spins that are different $(D(0) = 0.05)$.

As we will see in the next section, in some situations we need to compare the evolution of *three* distinct replicas A, B and C. In this case, we use the following set of initial configurations:

(d) same as in (b) and configuration $\{\sigma_i^C(0) \neq \sigma_i^A(0)\forall_i\}$ where each spin of replica C is given any of the two other possible states with equiprobability $(D_{AB}(0) = \frac{1}{2}$ and $D_{AC}(0) = 1)$.

3. Zero field results

3.1. Dynamical phase diagram

In figure 1 we show the survival probability, $P(t)$, as a function of temperature, T, for set (c) of the initial configurations at different times, t, examining samples of linear size $L = 64$. First, notice that, at $t = 10\,000$, $P(t)$ has already achieved a stationary value for this size. In view of its temperature dependence, we clearly observe *three* distinct regimes: (i) a low-temperature regime (for $T < T_2$, with $T_2 \simeq 1.0$) where P varies in a non-abrupt way with T; (ii) an intermediate regime (for $T_2 \leqslant T < T_1$, with $T_1 \simeq 1.2$) where $P = 1$ for

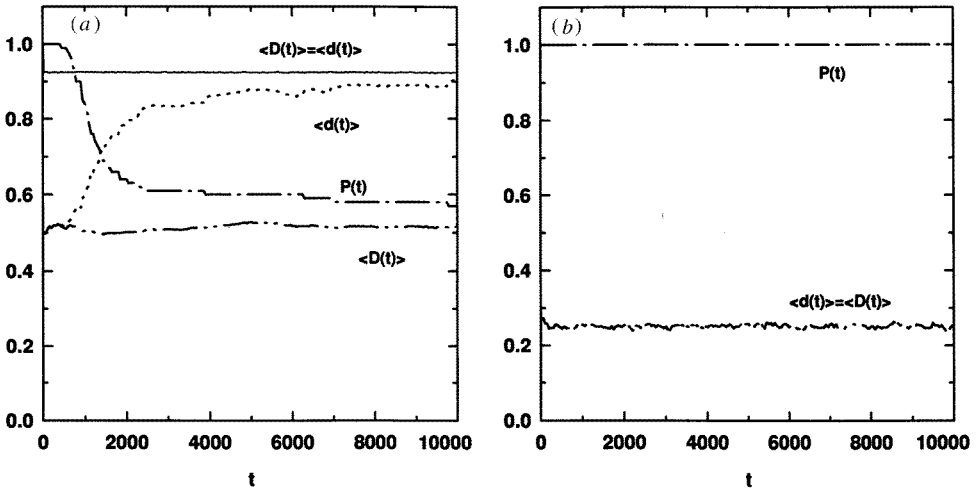

Figure 2. Time evolutions of $\langle D(t)\rangle$ (— · · —) $\langle d(t)\rangle$ (· · · · · ·) and the survival probability $P(t)$ (— · —) for the fixed temperatures (*a*) $k_BT/J = 0.90$ and (*b*) $k_BT/J = 1.06$. The simulations were performed on $M = 100$ samples of linear size $L = 64$ with set (b) of the initial conditions ($D(0) = \frac{1}{2}$). In (*a*), we also represent by a full line, the results for an initial damage $D(0) = 1$ (set (a) of the initial configurations) where $\langle D(t)\rangle = \langle d(t)\rangle$ since $P(t) = 1$ in this case.

all T; and (iii) a high-temperature regime (for $T \geqslant T_1$) where $P = 0$. Similar behaviours (not presented herein) are obtained for other sizes ($L = 16$, 32 and 128) and for set (b) of the initial configurations. The abrupt variations of P near T_1 and T_2 indicate the existence of dynamical transitions at these temperatures. Leroyer and Rouidi [12] observed a similar behaviour, starting from $D(0) = 1$, in the two higher transition temperatures (see [12, figure 9]) of the p-state clock model ($5 \leqslant p \leqslant 10$). This is in contrast to the behaviour found for the 3D Ising ferromagnet [2] where P, for any fixed $D(0)$, decreases slowly with an increasing T until it vanishes at the critical temperature.

In figures 2 we exhibit the temporal behaviours of $P(t)$, $\langle d(t)\rangle$ and $\langle D(t)\rangle$ for fixed temperatures using set (b) of the initial configurations. For a temperature $T = 0.90 < T_2$, we see from figure 2(*a*) that all these three quantities remain more or less stationary during the first MCS (roughly around 500 MCS) and afterwards vary during a transient time interval, Δt_0, until they fluctuate around non-zero stationary values. We observed similar behaviours (not presented herein) for other values of $T < T_2$ and, as the temperature increases towards the transition temperature T_2, the time Δt_0 becomes longer and longer. For comparison, we also present in figure 2(*a*) $\langle d(t)\rangle$ (full line) for set (a) of the initial configurations: this line coincides with $\langle D(t)\rangle$ since we have observed in our numerical simulations that, for $D(0) = 1$, $P(t)$ equals 1. Notice that $\langle d(t)\rangle$ for both sets (a) and (b) of the initial conditions seem to converge to the same long-time limit, while this fact does not occur with the damage $\langle D(t)\rangle$. Therefore, $\langle d(t)\rangle$ is not a convenient distance for studying the evolution of the two replicas for $T < T_2$ since, if one waits for a sufficient long but finite time, one will not see the low-temperature regime (i). In other words, in this situation T_2 would tend to zero as it happened in the Ising ferromagnet [2] whose temperature behaviour of $P(t)$ has only *two*, instead of three regimes.

For $T = 1.06$, one can see from figure 2(*b*) that the transient interval, Δt_0, is very small (Δt_0 is roughly 100 MCS) and $P(t)$ equals 1, leading thus to the equality $\langle d(t)\rangle = \langle D(t)\rangle$. As we change the temperature in this intermediate regime ($T_2 \leqslant T < T_1$), we obtain

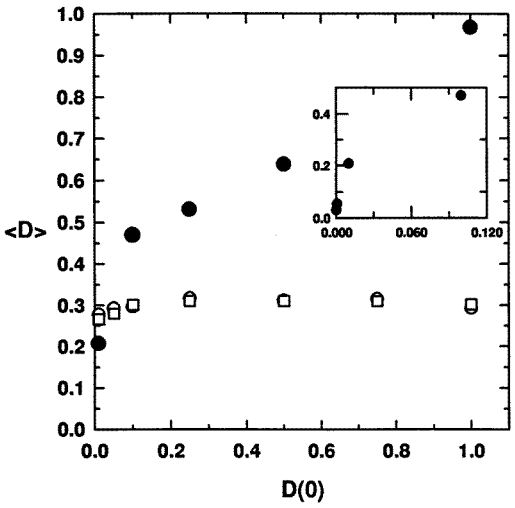

Figure 3. Plot of $\langle D(t = 10\,000)\rangle$ versus the initial damage $D(0)$ for the fixed temperatures $k_BT/J = 0.80$ (represented by full dots) and $k_BT/J = 1.04$ (represented by empty dots). The results for $t = 1000$ are also shown (by squares) when $T = 1.04$. We performed the averages over $M = 20$ samples of size $L = 64$ at $k_BT/J = 1.04$, while the number of replicas varied from 50 to 1000 at the other temperature. The inset shows the results for $k_BT/J = 0.80$ in the region near $D(0) = 0$.

(not shown herein) a similar behaviour, with Δt_0 increasing as we approach T_1. In this whole temperature regime the simulations remain unaltered if we use other sets of initial configurations, showing that both $\langle D(t)\rangle$ and $\langle d(t)\rangle$ become independent of $D(0)$ and that $P(t) = 1$ in this region.

In the high-temperature regime (iii) (for $T \geqslant T_1$), our simulations (not exhibited herein) show that $P(t)$, $\langle d(t)\rangle$ and $\langle D(t)\rangle$ fall off to zero after a transient time interval, Δt_0, which decreases rapidly to zero as we increase the temperature difference between T and T_1.

For the reasons given above, we will henceforth focus our attention exclusively to quantities which are averaged over *all* M samples, rather than over the M_1 configurations which have survived.

The sensibility of the long-time limit $\langle D\rangle$ to the initial conditions $D(0)$, for fixed temperatures, can be appreciated in figure 3. In the intermediate phase (illustrated for $T = 1.04$) $\langle D\rangle$ is independent of the initial non-zero $D(0)$, while the opposite happens in the low-temperature regime (illustrated for $T = 0.8$) where $\langle D\rangle$ is infinitesimally small for an infinitesimal $D(0)$ and increases almost to 1 as $D(0)$ becomes 1. Taking into account also that $P(t) = 1$ in the intermediate phase, we can thus say that this regime is *fully chaotic* in the sense that even two configurations infinitesimally close at $t = 0$ will always become separated by a *finite* distance.

The three temperature regimes can be also seen in the plot of $\langle D(t)\rangle$ as a function of T, for different initial conditions, exhibited in figure 4. We observe the following: (i) for $T < T_2$, $\langle D(t)\rangle$ is non-zero and depends upon the initial $D(0)$; (ii) for $T_2 \leqslant T < T_1$, $\langle D(t)\rangle$ is non-zero and is independent of the initial $D(0)$ and (iii) for $T \geqslant T_1$, $\langle D(t)\rangle = 0$ for any initial $D(0)$. This plot corresponds to simulations performed for $L = 64$, $M = 100$ samples and $t = 10\,000$. The same figure is obtained for $500 \leqslant t < 10\,000$ except in the neighbourhoods of T_1 and T_2, indicating that outside these small temperature ranges $\langle D(t)\rangle$ seems to have already reached its long-time limit $\langle D\rangle$. In view of the system size

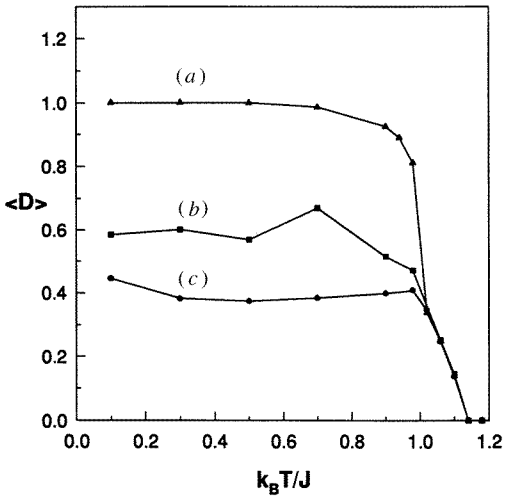

Figure 4. Average damage $\langle D \rangle$ versus temperature for three different initial damages (*a*) $D(0) = 1$, (*b*) $D(0) = 0.5$ and (*c*) $D(0) = 0.05$. Simulations were performed for $M = 100$ samples of linear size $L = 64$ and $t = 10\,000$.

dependence, $\langle D \rangle$ does not vary much with L, the most accentuated differences occurring near the temperature transitions T_1 and T_2. The three-phase diagram that we obtained is similar to those found in the 3D spin glasses [2] and the 2D XY ferromagnet [6].

The low-temperature regime (i) is consistent with the known phase space structure of the ferromagnetic phase (three distinct valleys with the same energy but different magnetizations): two initial configurations far enough from each other in phase space (such that they are in different valleys at $t = 0$) will remain confined there and keep a finite distance for a long time. This distance presents memory effects (i.e. it remembers for a very long time the initial distance) and it increases monotonously with an increasing $D(0)$. The high-temperature regime (iii) can also be easily understood in terms of the phase space of the paramagnetic phase (one single valley): two configurations will always meet since they are in the same valley and, hence, the damage vanishes. But what is not clear is the phase space structure corresponding to the intermediate temperature regime (ii) where two distinct initial configurations keep a distance for a very long time (since $P(t) = 1$) and always achieve the same long-time distance for a fixed temperature, no matter how close they are at $t = 0$. Maybe this unusual behaviour could be due to a very flat phase space where any two configurations would evolve like two random walks in the phase space which, because of the high dimension, do not meet at reasonable times.

In view of the temperature dependence of the fluctuation $\sigma(t)$ (given by $\sqrt{\langle D^2(t) \rangle - \langle D(t) \rangle^2}$) of the average distance $\langle D \rangle$, our simulations (not exhibited herein) shows that, for set (a) of the initial conditions, there is an almost null fluctuation in the low-temperature regime, except near the transition (T_2) where it rises abruptly. A similar behaviour was detected, for $D(0) = 1$, in the lowest transition of the p-state clock model ($4 \leqslant p \leqslant 10$) [12]. In figure 5(*a*), we show a typical distribution of distances (after $t = 10\,000$) far from T_2, which has a unique peak at $D \simeq 1$ indicating that all pairs of configurations (which were initially in one of the ferromagnetic ground states) have fallen into different valleys in the free energy landscape. When the pairs of initial configurations are far from any of the ferromagnetic ground states, the fluctuation

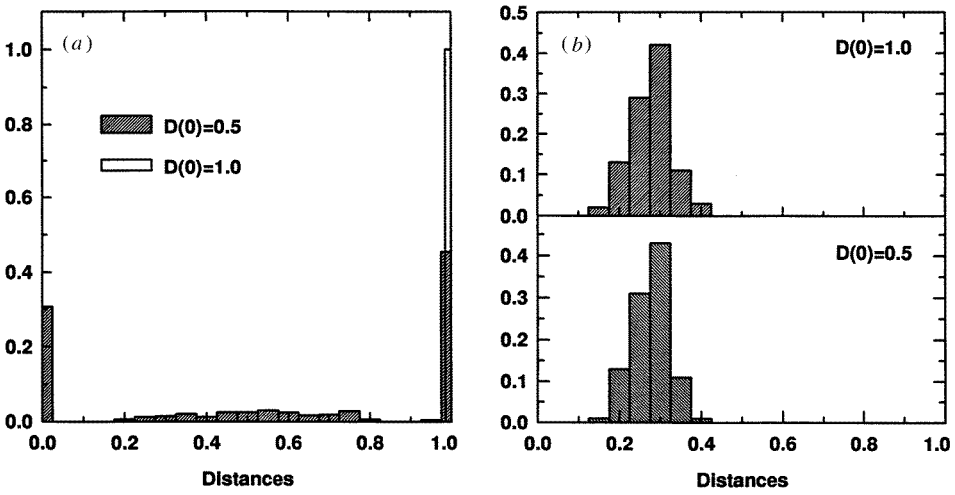

Figure 5. The distribution of distances after $t = 10\,000$ on a 64×64 lattice for set (a) ($D(0) = 1$) and set (b) ($D(0) = \frac{1}{2}$) of the initial configurations at temperatures (*a*) $T = 0.5$ and (*b*) $T = 1.06$. Simulations were performed for $M = 500$ samples at $T = 0.5$ and $M = 100$ at $t = 1.06$. We found, in (*a*) $\langle D \rangle \simeq 1.00$ and $\sigma \simeq 0.0005$ when $D(0) = 1$, and $\langle D \rangle \simeq 0.57$ and $\sigma \simeq 0.44$ when $D(0) = 0.5$. In (*b*) we obtained, for both initial conditions, $\langle D \rangle \simeq 0.25$ and $\sigma \simeq 0.04$.

$\sigma(t = 10\,000)$ is relatively large. This is due to the fact that the pairs which have a non-zero $D(t = 10\,000) \neq 1$ will still take a relatively long time (as T is not high) to jump the energy barriers among the valleys until they achieve either the same ($D = 0$) or different valleys ($D = 1$). The hatched histogram in figure 5(*a*) illustrates such a case for set (b) of the initial conditions and $T = 0.5$. As to the behaviour of σ in the intermediate temperature regime, we observed, for T not very near T_2, small fluctuations of $\langle D \rangle$ which decreases with an increasing temperature until it vanishes at T_1. Furthermore, the distribution of distances is *independent of the initial conditions*, as illustrated in figure 5(*b*) for sets (a) and (b) of the initial configurations. The fact that the system evolves with small fluctuations in the intermediate temperature regime has also been found in the unexpected phase of the p-state clock model ($5 \leqslant p \leqslant 10$) [12].

Since the finite time and size effects are more serious near the transition temperatures T_1 and T_2, we follow the finite size scaling procedure [4, 6, 17] in order to obtain more reliable estimates for these transition temperatures. For this, we first compute the following average quantities over M samples of linear size, L, at the temperature T:

$$\tau_1(L, T) = \frac{\sum_t t\langle D(L, T, t)\rangle}{\sum_t \langle D(L, T, t)\rangle} \tag{10}$$

$$\tau_2(L, T) = \frac{\sum_t t^2\langle D(L, T, t)\rangle}{\sum_t \langle D(L, T, t)\rangle} \tag{11}$$

and the ratio

$$\langle R(L, T)\rangle = \frac{\tau_2(L, T)}{\tau_1^2(L, T)} \tag{12}$$

where each sample, s, was iterated until its distance, D_s, had vanished. τ_1 and τ_2 are measures of average characteristic times for two configurations to meet, and both depend upon the size, L, and the temperature T.

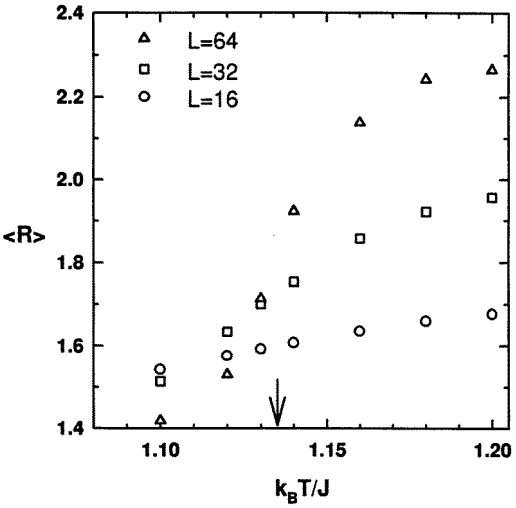

Figure 6. The ratio $\langle R\rangle = \langle \tau_2/\tau_1^2\rangle$ versus temperature for distinct sizes L. The number M of used samples was at most 16 000, 10 000 and 500 for $L = 16, 32$ and 64, respectively. The initial damage was $D(0) = 1$ (set (a) of the initial configurations). The error bars are smaller than the symbols. The arrow represents the exact static Ising critical temperature.

One expects the following finite size scaling forms for large L in the neighbourhood of the transition temperature T_1:

$$\tau_1(L,T) \approx u(L) f_1(v(L)(T - T_1)) \tag{13}$$

and

$$\tau_2(L,T) \approx u^2(L) f_2(v(L)(T - T_1)) \tag{14}$$

and consequently

$$\langle R(L,T)\rangle \approx f_3(v(L)(T - T_1)) \tag{15}$$

where $u(L)$ gives the size dependence at $T = T_1$ (usually $u(L)$ and $v(L)$ are power laws). We conclude from equation (15) that $\langle R(L,T)\rangle$ becomes independent of L at $T = T_1$. Therefore if we use sufficiently large sizes L_1, L_2, $L_3, \ldots$ their corresponding curves of $\langle R\rangle$ versus T should cross at the same temperature T_1. In figure 6 we show the plots of curves $\langle R(L,T)\rangle$, where we have used $L = 16, 32$ and 64 and set (a) of the initial conditions. From this we estimate that

$$\frac{k_B T_1}{J} = 1.13 \pm 0.01. \tag{16}$$

Other initial conditions would give different curves, but crossing at the same temperature given by (16). Notice that this value is unexpectedly close to the exact static critical temperature $k_B T_c(q = 2)/J = [\ln(1 + \sqrt{2})]^{-1} = 1.134\,59\ldots$ of the square lattice Ising ferromagnet.

In order to determine the other transition temperature, T_2, we follow the same procedure used for the XY model in [6]. Consider, thus, three different replicas A, B and C and define the following measure $\Delta(t)$ for comparing the evolution of $\{\sigma_i^A(t)\}$, $\{\sigma_i^B(t)\}$ and $\{\sigma_i^C(t)\}$ starting from chosen initial configurations $\{\sigma_i^A(0)\}$, $\{\sigma_i^B(0)\}$ and $\{\sigma_i^C(0)\}$:

$$\Delta(t) = D_{AC}(t) - D_{AB}(t). \tag{17}$$

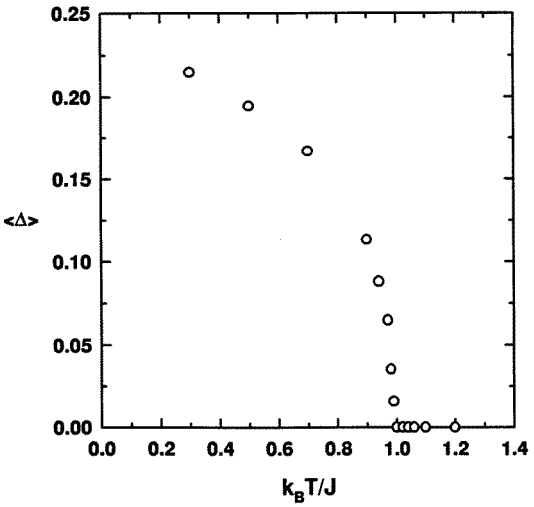

Figure 7. $\langle\Delta\rangle$ as a function of temperature. The simulations were performed at $t = 2000$ for $M = 200$ samples of size $L = 64$ with set (d) of the initial conditions.

The temperature dependence of the average $\langle\Delta(t)\rangle$ using set (d) of the initial conditions is shown in figure 7. From figure 7 we see that $\langle\Delta(t)\rangle$ for a sufficiently long time, t, plays the role of an order parameter for the continuous transition at T_2 similar to the role of $\langle D\rangle$ for the transition at T_1. We can thus characterize the three dynamical phases in terms of the two order parameters $\langle D\rangle$ and $\langle\Delta\rangle$ as (i) for $T < T_2$, $\langle D\rangle \neq 0$ and $\langle\Delta\rangle \neq 0$; (ii) for $T_2 \leqslant T < T_1$, $\langle D\rangle \neq 0$ and $\langle\Delta\rangle = 0$; (iii) for $T \geqslant T_1$, $\langle D\rangle = \langle\Delta\rangle = 0$.

Defining $\tau_1^{(\Delta)}(L,T)$, $\tau_2^{(\Delta)}(L,T)$ and $\langle R^{(\Delta)}(L,T)\rangle$ in a similar way to the respective equations (10)–(12), with $\langle D(L,T,t)\rangle$ being replaced by $\langle\Delta(L,T,t)\rangle$ (and iterating each sample until $\langle\Delta_s(L,T,t)\rangle$ vanishes for the first time) we obtain the temperature dependence of the average $\langle R^{(\Delta)}\rangle$ illustrated in figure 8. These curves cross at the temperature

$$\frac{k_B T_2}{J} = 0.99 \pm 0.01. \tag{18}$$

Notice that this estimate for the temperature transition T_2, below which $\langle D\rangle$ depends on the initial damage, is very close to the exact critical temperature $0.994\,97\ldots$ of the three-state Potts ferromagnet at thermal equilibrium. A similar observation has been made for the 3D spin glasses [2] and the 2D XY model [6].

3.2. Dynamical critical exponents

Similar to Wang *et al* [17], we compute the relaxation time critical exponents $z_1 \equiv z(T_1)$ and $z_2 \equiv z(T_2)$ (defined as $\tau \sim \xi^z$, where τ and ξ are the respective temporal and spatial correlation lengths) through the respective average time $\tau_1(L,T_1)$ and $\tau_1^{(\Delta)}(L,T_2)$ for $\langle D\rangle$ and $\langle\Delta\rangle$ to vanish, in other words, we suppose that

$$\tau_1\ (L,T_1) \sim L^{z_1} \tag{19}$$

and

$$\tau_1^{(\Delta)}(L,T_2) \sim L^{z_2}. \tag{20}$$

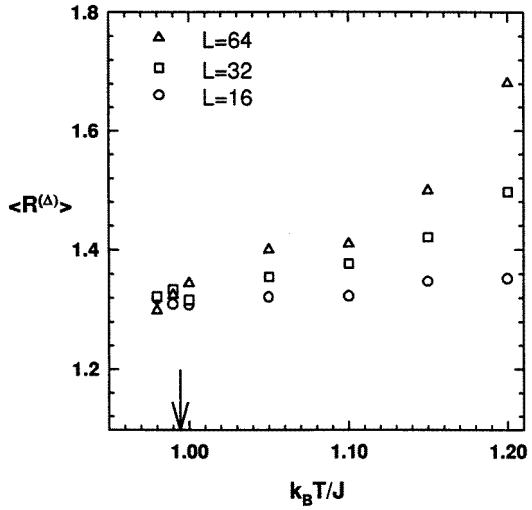

Figure 8. The ratio $\langle R^{(\Delta)}\rangle = \langle \tau_2^{(\Delta)}/(\tau_1^{(\Delta)})^2\rangle$ versus temperature for different sizes. We used at most $M = 10\,000$, 1000 and 250 replicas for the respective sizes $L = 16$, 32 and 64 with set (d) of the initial configurations. The error bars are smaller than the symbols. The arrow represents the exact static critical temperature T_c $(q = 3)$.

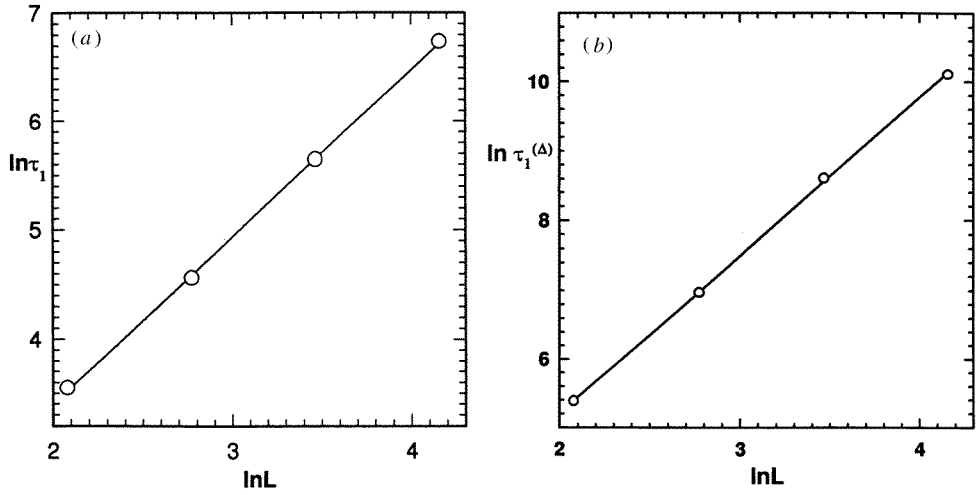

Figure 9. Log–log plots of the vanishing times (a) τ_1 and (b) $\tau_1^{(\Delta)}$ against the linear lattice size, L, calculated at the temperatures T_c $(q = 2)$ and T_c $(q = 3)$, respectively. In (a) we averaged over 16 000, 10 000, 4000 and 500 samples of respective linear sizes $L = 8$, 16, 32 and 64 with initial damage $D(0) = \frac{1}{2}$ (set (b) of the initial configurations). In (b) we used $M = 40\,000$, 20 000, 20 000 and 7000 of respective sizes $L = 8$, 16, 32 and 64 with set (d) of the initial conditions. The straight lines correspond to $z = 1.54$ (figure 8(a)) and $z = 2.28$ (figure 8(b)).

In figures 9(a) and (b) we present the respective log–log plots of τ_1 and $\tau_1^{(\Delta)}$ versus L, where the simulations were performed at the *exact* static critical temperatures T_c $(q = 2)$ and T_c $(q = 3)$ which we believe to be the exact values for T_1 and T_2. From the slope of the lines we estimate that

$$z_1 = 1.54 \pm 0.02 \tag{21}$$

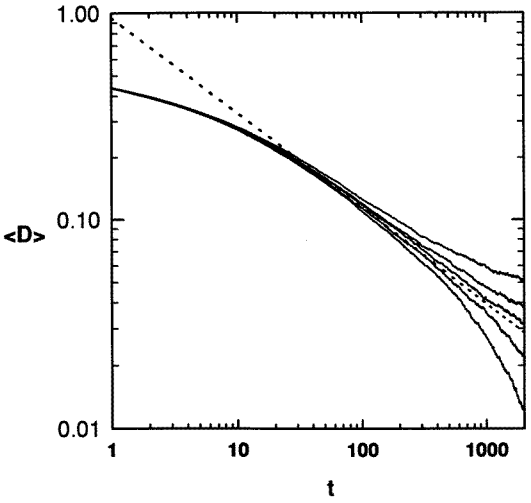

Figure 10. Log–log plot of $\langle D\rangle$ versus time, t, at the following fixed temperatures k_BT/J from top to bottom: 1.131, 1.1325, $k_BT_c(q=2)/J$ and 1.137. The results were averaged over 100 samples of linear size $L=256$ with initial damage $D(0)=1$ (configurations $\{\sigma_i^A(0)\}$ is random and configuration $\{\sigma_i^B(0)\} \neq \{\sigma_i^A(0)\}\forall i$). The broken curve (whose intercept is arbitrary) has the gradient -0.46 predicted from the directed percolation.

and

$$z_2 = 2.28 \pm 0.03. \tag{22}$$

Notice that z_2 compares well with the recent accurate value $z \simeq 2.196$ computed for the three-state Potts model from short-time dynamics [31] and with other previous results where $2.1 \leqslant z \leqslant 2.8$ (see [32] and references therein, [33]). In contrast, z_1 is far from the recent accurate value 2.172 ± 0.006 [19] and from other results ($1.9 < z < 2.3$) quoted in literature for the 2D Ising ferromagnet [32, 14, 17, 20, 21]. This indicates that the dynamic transition at T_1, although consistent with the static Ising critical temperature, is not in the Ising universality class since the damage spreading technique within the heat-bath dynamics has led, for the Ising model, to estimates for z [14, 17, 19–21] which agree with those derived from other methods. Notice that a similar discrepancy in the universality class also happens in the upper transition of spin glasses, where T_1 corresponds to the critical point of the bond-frustrated percolation and the critical exponents are in the standard bond percolation universality class [10, 34].

In figure 10 we present the temporal behaviour of $\langle D(t)\rangle$ for $L = 256$ at different temperatures in the range $1.131 \leqslant T \leqslant 1.137$. In the case of $T = T_c(q=2)$ we have also obtained $\langle D(t, L=128)\rangle$ (not shown herein) which, for $60 < t < 200$, becomes identical to $\langle D(t, L=256)\rangle$ and has a power law decay ($\langle D(t)\rangle \sim t^{-\delta}$) [4, 17–19]. In general $\langle D(t, L)\rangle$ is expected to follow [4], at $T = T_c$ and $t \gg 1$ and $L \gg 1$, the finite size scaling form $\langle D(t, L)\rangle \sim L^{-\delta z} f(t/L^z)$ where $f(x) \sim x^{-\delta}$ (for $x \ll 1$) leading thus, for $t \ll L^z$, to the above mentioned time decay. Therefore the time range $60 < t < 200$ over which our results for $\langle D(t, L)\rangle$ become size independent corresponds to the validity region of the power law decay $t^{-\delta}$. Taking this into account, from figure 10 we can extract an estimate for T_1 which has a better accuracy than that of equation (16), namely:

$$\frac{k_BT_1}{J} = 1.135 \pm 0.003. \tag{23}$$

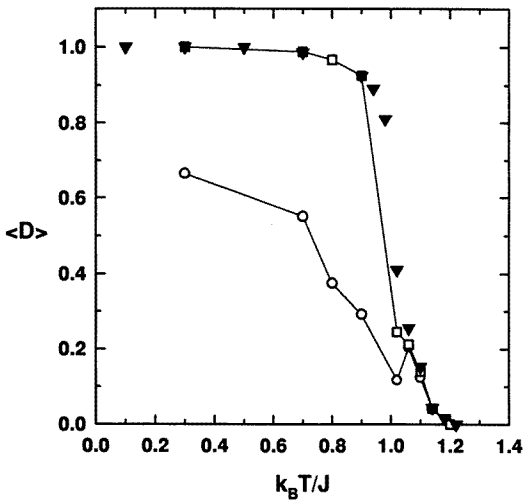

Figure 11. The average damage $\langle D(t = 10\,000)\rangle$ as a function of temperature for a magnetic field strength $B = 0.01$ and set (a) of the initial configurations (empty squares) and set (b) (empty circles). For comparison, we also represent (by full triangles) the results in a zero magnetic field with initial damage $D(0) = 1$. We used 200 samples of size $L = 64$.

From the slope of $\langle D(t)\rangle$ at $T = T_1$ in this time region we obtain that

$$\delta = 0.46 \pm 0.03 \tag{24}$$

which is compatible with the value $\delta \simeq 0.46$ for the directed percolation (DP) in $2 + 1$ dimensions (see [18] and references therein). A similar value was obtained in [18] where the spreading transition temperature disagrees with the static critical temperature. Our result (as well as that of [18]) supports Grassberger's conjecture [35] since the transition at T_1 does not coincide with the static three-state Potts one.

We have also examined the time evolution of $\langle\Delta(t)\rangle$ at temperatures around T_2. Our curves (not shown herein) also present a power law decay at $T = T_c$ ($q = 3$), but our statistics (2000 samples of size $L = 256$) was not sufficient for computing a reliable estimate of δ since in this case the survival probability of Δ is considerably smaller than 1 and the relaxation time is much larger ($\tau_1^{(\Delta)} \simeq 60\tau_1$for $L = 256$).

4. Influence of external fields

In figure 11 we illustrate the long-time $\langle D\rangle$ as a function of temperature, T, when a magnetic field of strength $B = 0.01$ (see equation (1)) is applied. The simulations were performed for set (a) of the initial conditions (represented by squares) and set (b) (represented by circles). For comparison, we also include points (represented by triangles) corresponding to a zero-field and set (a) of the initial configurations. From this we see that both transitions persist under the application of a small magnetic field (notice that for a sufficiently large field $\langle D\rangle$ vanishes for all T), similar to the 2D [18] and 3D [7, 18] Ising ferromagnets with Glauber dynamics. Consequently *the magnetic field is neither the conjugate field associated with the order parameter* $\langle D\rangle$ *nor that associated with* $\langle\Delta\rangle$.

A new kind of external field, h, was introduced a few years ago [28], in the context of the Domany–Kinzel cellular automaton (see [36]), which destroys the damage transition

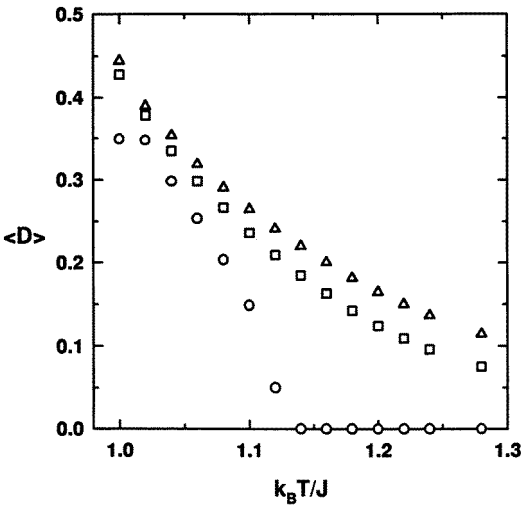

Figure 12. The temperature dependence of $\langle D(t = 4100)\rangle$ for different values of the external field h. We used $M = 100$ samples of linear size $L = 64$ with set (b) of the initial configurations.

and leads to the divergence of its associated susceptibility.

$$\chi_h \equiv \frac{\partial\langle D\rangle}{\partial h}|_{h\to 0} \tag{25}$$

at the transition. They defined h as *the frequency at which distinct random numbers are used to update the two replicas*, weakening thus the coupling between the replicas. A mean-field analysis [29] of this cellular automaton predicted the same type of behaviour for χ_h. More recent numerical simulations of the damage spreading on the 2D Ising ferromagnet [15] also show that h plays the role of a conjugate field to the Hamming distance $\langle D(t)\rangle$.

The results of the application of such an external field h (for $h = 0.005$ and $h = 0.010$) are exhibited in figure 12; for comparison $\langle D(t)\rangle$ for $h = 0$ is also shown. One can clearly see that a small h destroys the continuous damage spreading transition observed for $h = 0$ at $T = T_1$. Since there is no analogue with the fluctuation-dissipation theorem for the damage, we obtain an approximation for the zero-field susceptibility, χ_h, by calculating the variation of the damage $\langle D(t)\rangle$ corresponding to a small change of h. Figure 13 displays these approximations for χ_h versus T for the above values of the field. We observe, similar to the 2D Ising ferromagnet [15], a tendency for χ_h to diverge near the corresponding transition temperature T_1 as $h \to 0$, indicating thus that h is the conjugate field $\langle D\rangle$. In view of the other transition at T_2, the situation is more complicated since it involves the comparison of three replicas. If one defines h as, for example, the frequency at which distinct random numbers are used to update the *three* replicas, then the application of a small h increases $\langle\Delta\rangle$ at any fixed temperature $T < T_2$, but it does not prevent $\langle\Delta\rangle$ vanishing above a certain temperature. We have also tried other similar definitions for h, but we have not succeeded in finding a conjugate field to $\langle\Delta\rangle$.

5. Conclusions

The dynamical behaviour of the three-state Potts ferromagnet on the square lattice is investigated through the damage spreading method within the heat-bath dynamics. We

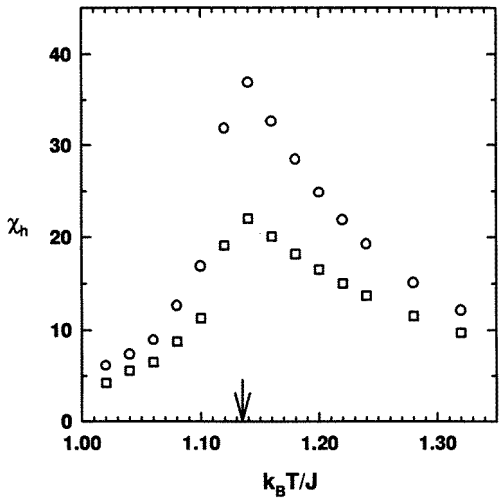

Figure 13. Approximations for the susceptibility χ_h (defined in equation (5)) versus temperature obtained from the results of figure 11. The arrow represents the exact static Ising critical temperature T_c $(q = 2)$.

found that this is the simplest spin model studied so far which presents a three-phase structure similar to that encountered in more complex systems, such as the 3D spin glasses [2, 10] and the 2D XY ferromagnet [5]. Furthermore, the unexpected chaotic phase which appears above the static Potts critical temperature $T_2 = T_c(q = 3)$ and below the static Ising one $T_1 = T_c$ $(q = 2)$ has unusual features. In this phase, two initial configurations remain different for a very long time (since the survival probability, $P(t)$, equals 1) and always achieve, for a fixed temperature, the same long-time Hamming distance no matter how close they are at $t = 0$. Maybe this is due, in terms of free energy landscape, to an extensive flattening where any two configurations would evolve like two random walks which do not cross at reasonable times because of the high dimensionality of the phase space. Another odd result concerning the new phase was obtained, namely: despite its upper boundary T_1 occurs, within the error bars, at $T_c(q = 2)$, its corresponding dynamic critical exponent z_1 differs a lot from the reported values for the Ising model. The short-time decay exponent, δ, of the Hamming distance indicates that this transition is in the $(2 + 1)$-dimensional directed percolation universality class, in agreement with Grassberger's conjecture [35]. We have also verified that the new kind of external field, h, introduced a few years ago [28] plays the role of a conjugate field to the order parameter $\langle D \rangle$ of this transition, i.e. it destroys the transition at T_1 observed at $h = 0$ and its associated susceptibility diverges at T_1.

It would be interesting to investigate the long-time behaviour of the spin auto-correlation function, $C(t)$, in each of the three dynamical phases in order to see, in particular, how its functional form in the low-temperature regime differs from that of the intermediate one. Since we found that the relaxation time at T_1 is smaller than at T_2 (as $z_1 < z_2$) and that the memory effect of the initial damage disappears for $T \geqslant T_2$, we expect that (similar to the 3D spin glasses [23, 24]) $C(t)$ in the intermediate phase decays slower than in the high-temperature regime (where it is probably given by a simple exponential decay) but faster than in the low-temperature one (where it could be eventually given by a stretched exponential decay similar to that found for the 2D Ising ferromagnet [37, 22]). Work along this line is in progress.

Further studies are needed to clarify the real nature of the unexpected phase. In particular, remaining uncertainties involve checking whether its upper boundary T_1 is exactly equal to T_c ($q = 2$) and, in the affirmative case, it would be very interesting to understand the profound reasons for this coincidence.

Acknowledgments

We acknowledge C Tsallis and E M F Curado for fruitful discussions. We thank CNPq and VITAE Foundation for financial support. Simulations were carried out on a CRAY J90 of NACAD-COPPE/UFRJ and on a CRAY YMP of CESUP/UFRGS.

References

[1] Costa U M S 1987 *J. Phys. A: Math. Gen.* **20** L583
[2] Derrida B and Weisbuch G 1987 *Europhys. Lett.* **4** 657
[3] Barber M N and Derrida B 1988 *J. Stat. Phys.* **51** 877
[4] Newmann A U and Derrida B 1988 *J. Physique* **49** 1647
[5] Golinelli O and Derrida B 1988 *J. Physique* **49** 1663
[6] Golinelli O and Derrida B 1989 *J. Phys. A: Math. Gen.* **22** L939
[7] Le Caer G 1989 *J. Phys. A: Math. Gen.* **22** L647
Le Caer G 1989 *Physica* **159A** 329
[8] Chiu J and Teitel S 1990 *J. Phys. A: Math. Gen.* **23** L891
[9] Mariz A M 1990 *J. Phys. A: Math. Gen.* **23** 979
Nobre F D, Mariz A M and Sousa E S 1992 *Phys. Rev. Lett.* **69** 13
[10] De Arcangelis L 1990 *Correlations and Connectivity* ed H E Stanley and N Ostrowsky (Dordrecht: Kluwer)
[11] Golinelli O 1990 *Physica* **167A** 736
[12] Leroyer Y and Rouidi K 1991 *J. Phys. A: Math. Gen.* **24** 1931
[13] Miranda E N and Parga N 1991 *J. Phys. A: Math. Gen.* **24** 1059
[14] Stauffer D 1993 *J. Phys. A: Math. Gen.* **26** L599
[15] Tamarit F A and da Silva L 1994 *J. Phys. A: Math. Gen.* **27** L809
[16] Tamarit F A and Curado E M F 1994 *J. Phys. A: Math. Gen.* **27** 671
[17] Wang F, Hatano N and Suzuki M 1995 *J. Phys. A: Math. Gen.* **28** 4543
[18] Grassberger P 1995 *J. Phys. A: Math. Gen.* **28** L67
[19] Grassberger P 1995 *Physica* **214A** 547
Grassberger P 1995 *Physica* **217A** 227 (erratum)
[20] Gropengiesser U 1995 *Physica* **215A** 308
[21] Wang F and Suzuki M 1996 *Physica* **223A** 34
[22] Grassberger P and Stauffer D 1996 *Physica* **232A** 171
[23] Ogielski A T 1985 *Phys. Rev.* B **32** 7384
[24] Campbell I A 1986 *Phys. Rev.* B **33** 3587
[25] Wu F Y 1982 *Rev. Mod. Phys.* **54** 235
Tsallis C and de Magalhães A C N 1996 *Phys. Rep.* **268** 305
[26] Bibiano M F A, Moreira F B and Mariz A M Damage spreading in the q-state Potts model *Preprint*
[27] Palandi J, de Almeida R M C and Iglesias J R Private communication
[28] Tsallis C and Martins M L 1994 *Europhys. Lett.* **27** 415
[29] Tomé T 1994 *Physica* **212A** 99
[30] da Silva L, Tamarit F A and de Magalhães A C N 1997 *Europhys. Lett.* in press
[31] Schülke L and Zheng B 1995 *Phys. Lett.* A **204** 295
[32] Tang S and Landau D P 1987 *Phys. Rev.* B **36** 567
[33] Aydin M and Yalabik M C 1988 *J. Phys. A: Math. Gen.* **21** 769
Aydin M and Yalabik M C 1984 *J. Phys. A: Math. Gen.* **17** 2531
Aydin M and Yalabik M C 1985 *J. Phys. A: Math. Gen.* **18** 1741
[34] De Arcangelis L, Coniglio A and Peruggi F 1991 *Europhys. Lett.* **14** 515
[35] Grassberger P 1995 *J. Stat. Phys.* **79** 13
[36] Martins M L, de Resende H F V, Tsallis C and de Magalhães A C N 1991 *Phys. Rev. Lett.* **66** 2045
[37] Huse D A and Fisher D S 1987 *Phys. Rev.* B **35** 6841